Laboratory of Computational Physics

by Luca Cassia

Dipartimento di Fisica, Università di Milano-Bicocca
I-20126 Milano, Italy

Email: l.cassia@campus.unimib.it

Table of contents

1 Potts Model 2*d*

The 2-dimensional Potts Model constitutes a generalization of the Ising Model to a generic number $q \in \mathbb{N}$ of states for the spin variable. A useful way to picture the space of states of a Potts spin variable is to map it to the space $U(1) \subset \mathbb{C}$ of unimodular complex numbers. We represent each state p with the p^{th} complex q-root of the unity in $\mathbb{C}$:

$$p \mapsto e^{\frac{2\pi i}{q} p} \in U(1) \tag{1}$$

Lets consider a 3-state Potts system of $L \times L$ spins situated on the points of a regular square lattice with periodic boundary conditions (PBC) in both directions, as for the Ising Model. Each spin interacts with its nearest neighbours inside the lattice, with an Hamiltonian:

$$\mathcal{H} = -\sum_{\langle i,j \rangle} \delta_{\sigma_i,\sigma_j} \tag{2}$$

where the sum is taken only over the set of unordered pairs $\langle i, j \rangle$ such that σ_i and σ_j are nearest neighbours. The implementation of the MH algorithm is completely analogous to that for the ising model, while for the SW algorithm we need to modify the probability with which to activate the link between neighbouring spins. In fact, the partition function can be written as:

$$Z[\beta] = \sum_{\{\sigma\}} \mathrm{e}^{\beta \sum_{\langle ij \rangle} \delta_{\sigma_i \sigma_j}} = \sum_{\{\sigma\}} \prod_{\langle ij \rangle} \mathrm{e}^{\beta \delta_{\sigma_i \sigma_j}} \tag{3}$$

using the Fortuin-Kasteleyn representation we can write:

$$\mathrm{e}^{\beta \delta_{\sigma_i \sigma_j}} = 1 + (\mathrm{e}^{\beta} - 1)\delta_{\sigma_i \sigma_j} = \mathrm{e}^{\beta} \left[\mathrm{e}^{-\beta} + (1 - \mathrm{e}^{-\beta})\, \delta_{\sigma_i \sigma_j}\right] \tag{4}$$

therefore we can immediately read the probability of establishing a link between neighbouring spins as:

$$p = 1 - \mathrm{e}^{-\beta} \tag{5}$$

1.1 Thermalization

As for the case of the Ising Model, we opted for a cold start approach. In (Fig.1) we present the thermalization process for MH and SW at various temperatures and for two different volumes: 32^2 and 64^2. The observed quantity is the energy density:

$$e = \langle \mathcal{H} \rangle / V \tag{6}$$

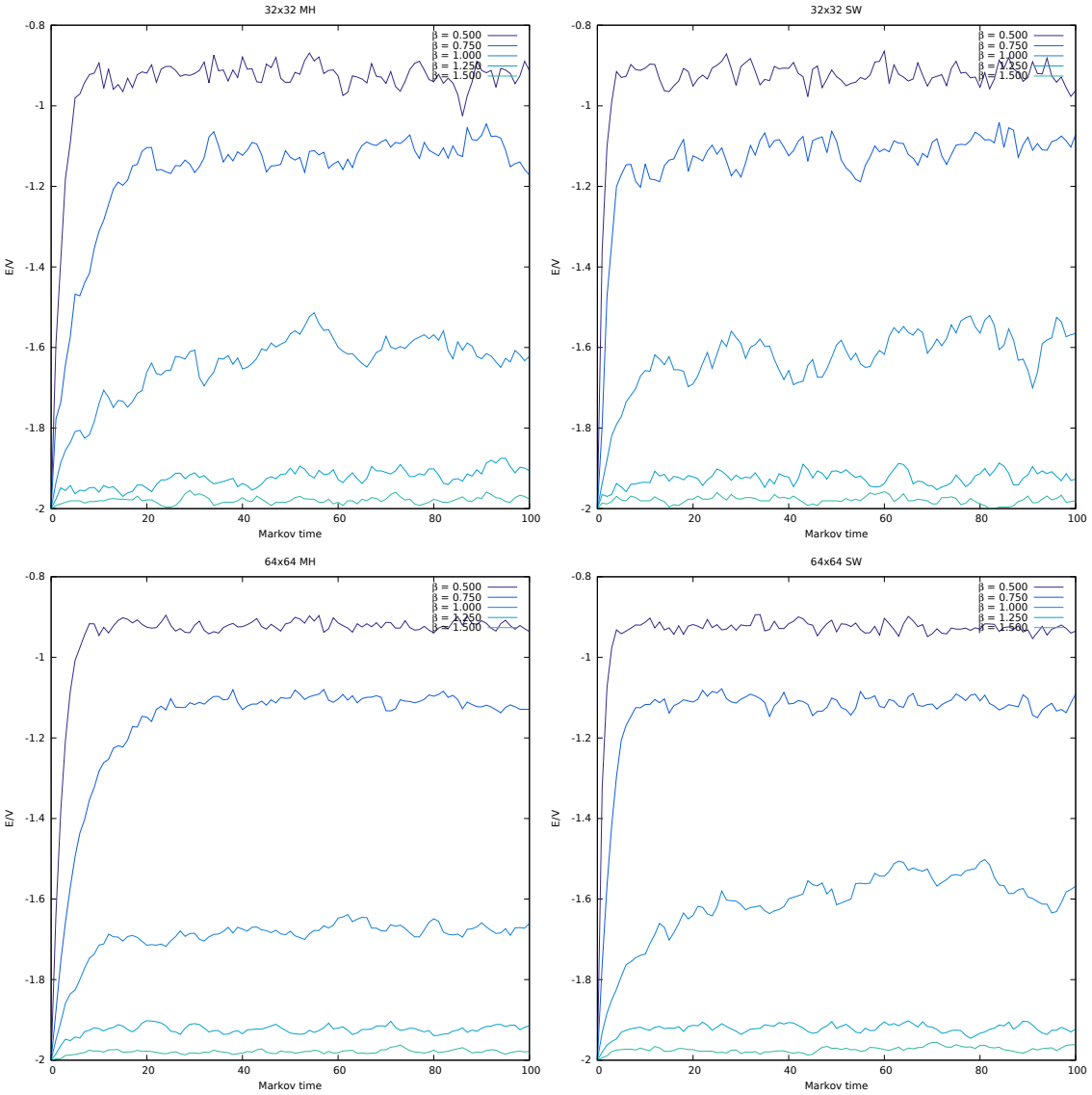

Figure 1. Thermalization process of the energy density on a lattice 32×32 in the top two pictures and 64×64 in the bottom two. MH on the left, SW on the right.

As expected, the MH algorithm has a slower mixing rate due to the critical slowing down effect near the critical inverse temperature:

$$\beta_c = \log\left(1+\sqrt{3}\right) \approx 1.00505254... \tag{7}$$

For this reason we focus only on the study of the model through the implementation of the much more efficient SW algorithm. The thermalization time is taken to be 1000 Markov steps.

1.2 Autocorrelation Times

We now study the correlations present in the energy density signal produced by the Markov process. As we did for the Ising Model, we fit the data using the integrated autocorrelation time exact result for a bivariate gaussian signal:

$$\tau_{\text{int}}(k_{\max}) = \tau_{\text{int}}\left[1 - \frac{2\,\tau_{\text{exp}}}{2\,\tau_{\text{exp}}+1}\,\mathrm{e}^{-k_{\max}/\tau_{\text{exp}}}\right] \tag{8}$$

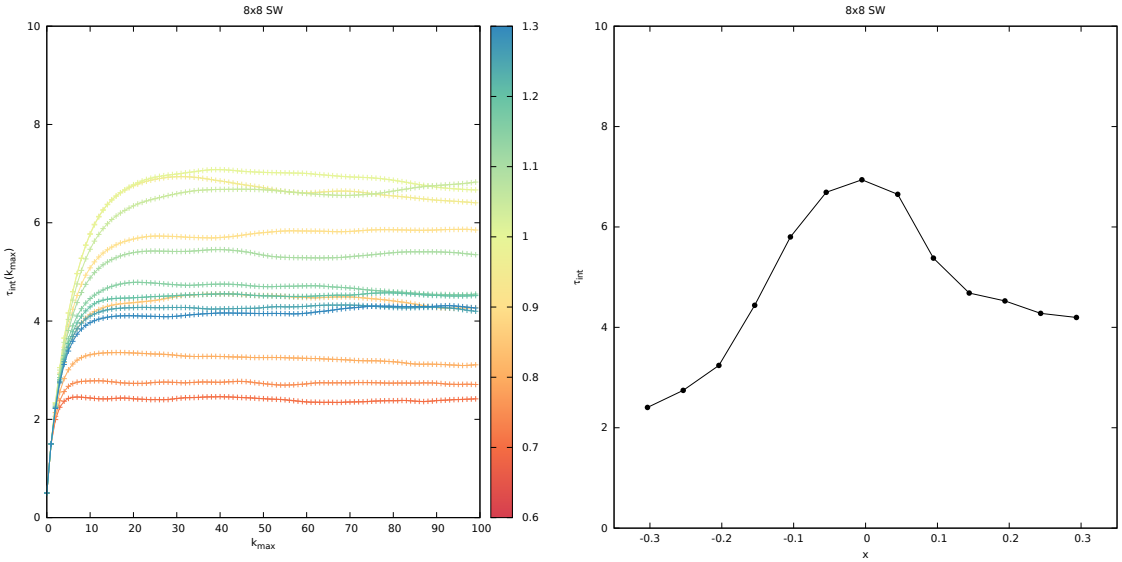

Figure 2. Plots of the autocorrelation of the signal for e. On the left is shown the integrated autocorrelation time τ_{int} as a function k_{max}. The chromatic scale indicates the value of β. On the right is shown the plot of τ_{int} as a function of $x = \frac{\beta - \beta_c}{\beta_c}$. The lattice size is $L = 8$.

As already pointed out, the autocorrelation time of the SW signal is very low even near the phase transition because of the dynamical critical exponent $z \approx 0$. Thus we can safely set the bin size to 50.

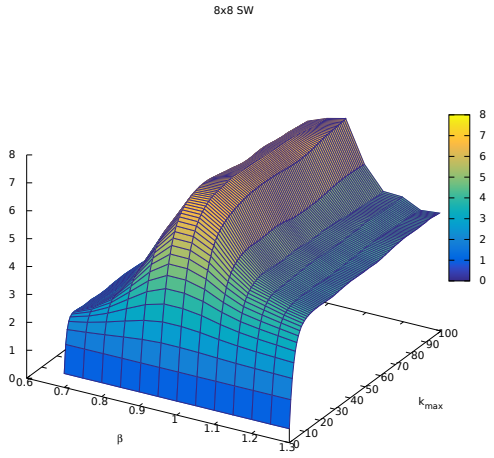

Figure 3. 3d plot of $\tau_{\mathrm{int}}(\beta, k_{\mathrm{max}})$ for a Potts Model of volume 8×8 near β_c.

1.3 Observables

The main observables of interest for this system are the energy density e and the magnetization m:

$$e = \langle \mathcal{H} \rangle / V, \tag{9}$$

$$m = \langle |\mathcal{M}| \rangle, \qquad \mathcal{M} = \frac{1}{V} \sum_i \sigma_i \tag{10}$$

For each inverse temperature we compute the estimate of the generic observable $\mathcal{O}$ from a set of $5 \cdot 10^4$ measurements.

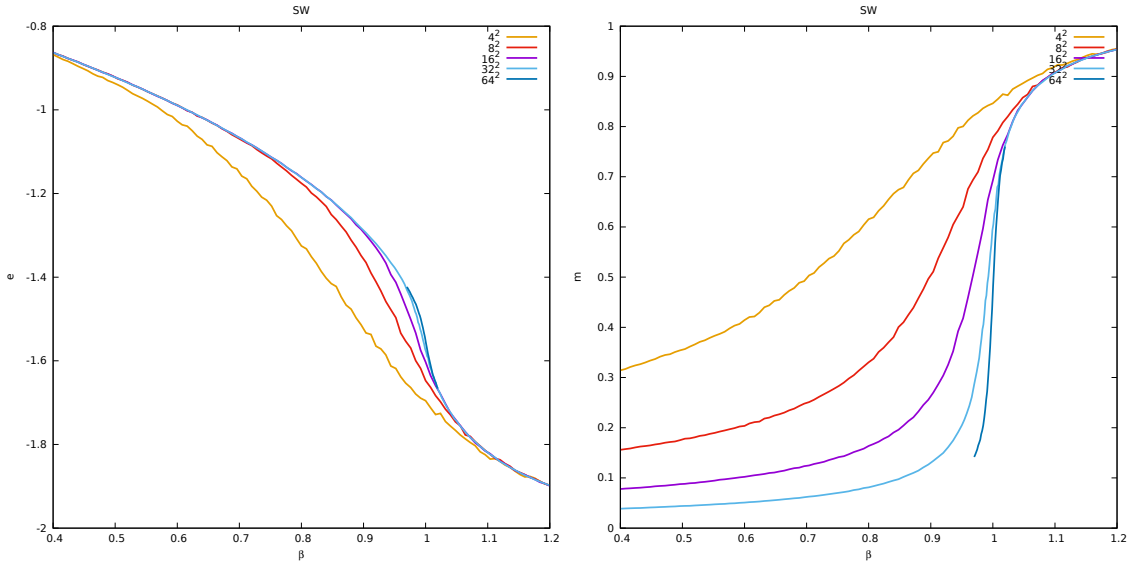

Figure 4. Left: energy density e as a function of β. Right: magnetization modulus m. The various colors represent different lattice sizes: $L = 4, 8, 16, 32$.

As the lattice volume $V = L^2$ increases, both the energy and magnetization curves approach their infinite volume limit.

We also plot the heat capacity and the magnetic susceptibility:

$$C = \frac{\beta^2}{V} \langle (\mathcal{H} - \langle \mathcal{H} \rangle)^2 \rangle \tag{11}$$

$$\chi = \beta V \langle (|\mathcal{M}| - \langle |\mathcal{M}| \rangle)^2 \rangle \tag{12}$$

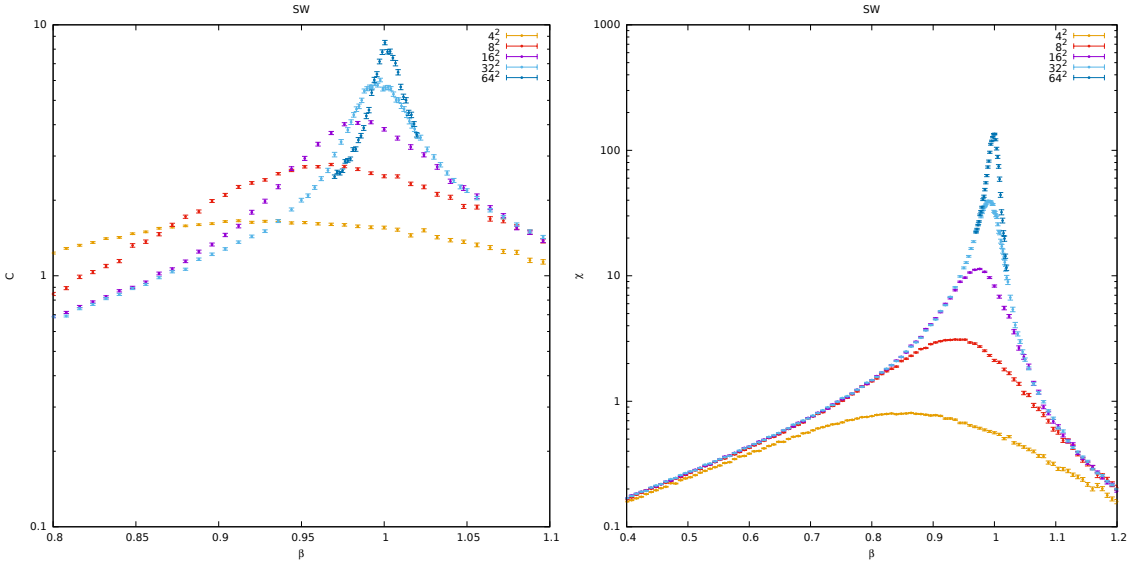

Figure 5. Left: heat capacity as a function of β. Right: magnetic susceptibility. The various colors represent different lattice sizes: $L = 4, 8, 16, 32, 64$.

1.4 β Critical

From a power law fit of the points near the peak of each dataset we obtain estimates for the pseudocritical β-values at finite sizes $L = 4, 8, 16, 32, 64$.

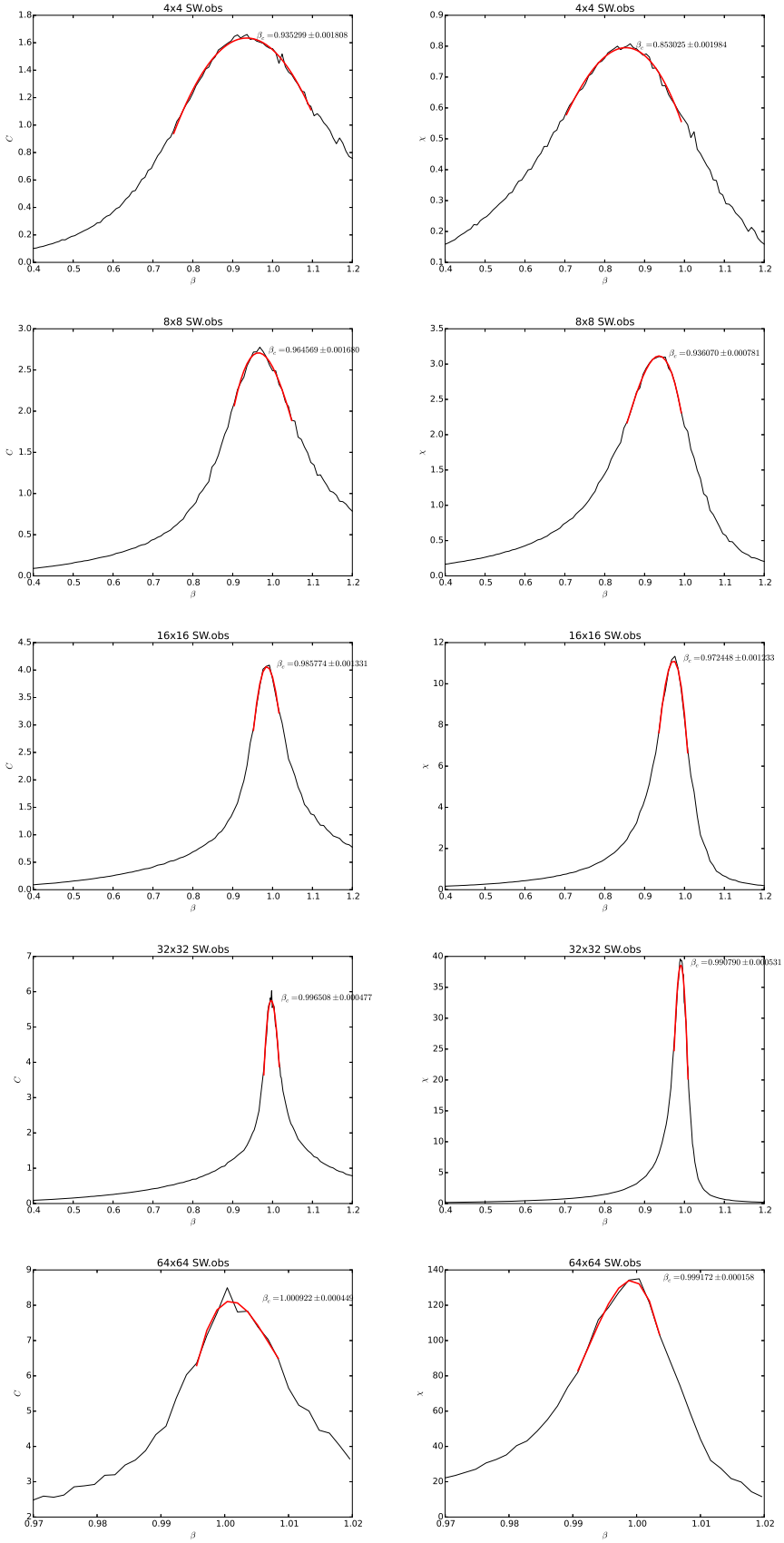

Figure 6. Fit of the heat capacity and susceptibility peaks.

L	$\beta_{\max}(C)$	$\beta_{\max}(\chi)$
4	0.93530 ± 0.00181	0.85303 ± 0.00198
8	0.96457 ± 0.00168	0.93607 ± 0.00078
16	0.98577 ± 0.00133	0.97245 ± 0.00123
32	0.99651 ± 0.00048	0.99079 ± 0.00053
64	1.00092 ± 0.00045	0.99917 ± 0.00016

Table 1. Pseudocritical β-values obtained by polynomial fit of the peaks of C and χ.

The polynomial function we used for the fit is:

$$f(\beta) = A + B\,(\beta - \beta_{\max})^2 + C\,(\beta - \beta_{\max})^3 \tag{13}$$

We can now obtain an estimate of β_c from a power law fit to the location of the maxima $\beta_{\max}$:

$$\beta_{\max} = \beta_c - c\,L^{-\nu} \tag{14}$$

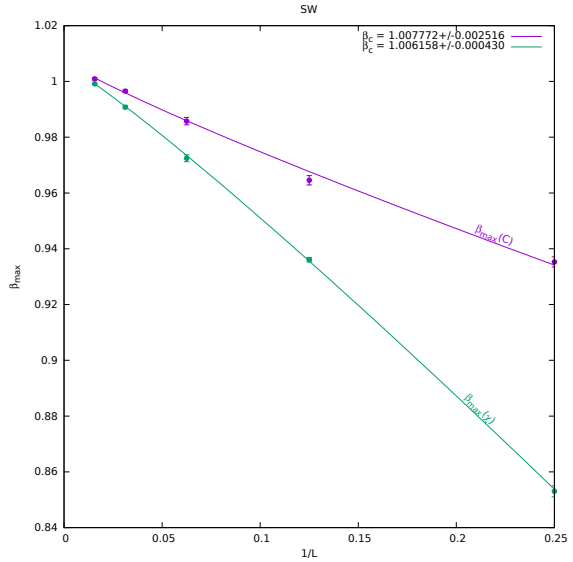

Figure 7. Pseudocritical inverse temperature fit. The purple lines are relative to the heat capacity C while the green ones to the magnetic susceptibility χ.

The result of the fit are:

$$\beta_c(C) = 1.00777 \pm 0.00252 \tag{15}$$

$$\beta_c(\chi) = 1.00616 \pm 0.00043 \tag{16}$$

As we can see, both values obtained from the fit of C and χ are very close to the exact solution of (7). We could improve these results further by discarding some measurements done at smaller volumes ($L = 4$ and $L = 8$ for instance) and repeat the measurement procedure for larger lattice sizes.

1.5 Probability Distribution Functions

We study the probability distribution of the magnetization for a lattice of size $L = 8$. The energy and magnetization levels of a discrete system are quantized. In particular, for a Potts Model on a square lattice of size L^2 with PBC, there are exactly $\frac{1}{2}(L^2+1)(L^2+2)$ magnetization levels distributed as in (Fig.8):

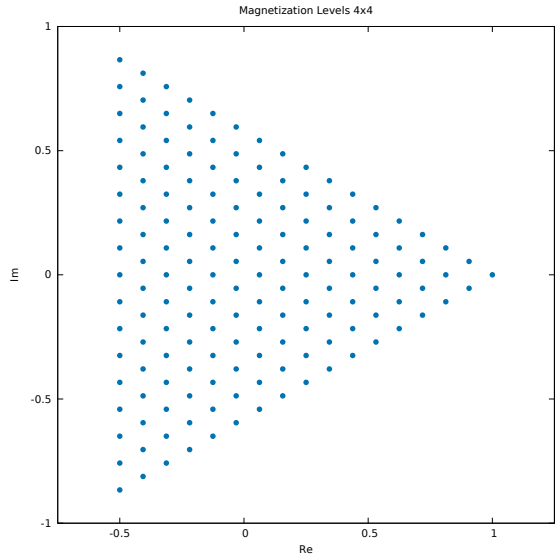

Figure 8. Magnetization levels of the Potts Model on a 4×4 lattice. We remark that, since the average is a convex function of its arguements, every magnetization level must be contained in the convex hull of the three basic magnetizations $1, \frac{-1+i\sqrt{3}}{2}, \frac{-1-i\sqrt{3}}{2}$ (*magnetization domain*).

With this consideration one can construct the probability distribution function of the magnetization just by counting the number of samples in each level (for L not too large):

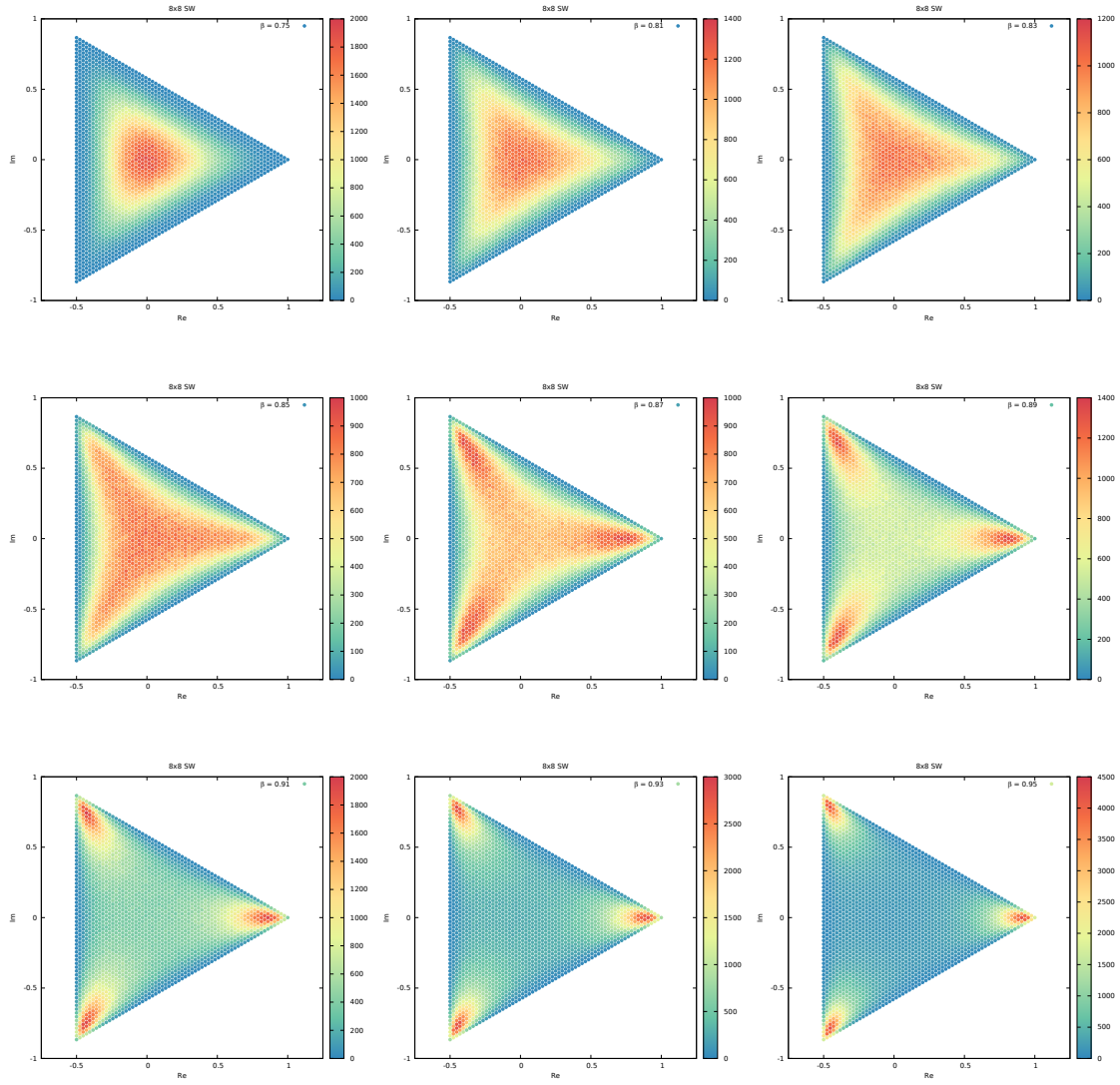

Figure 9. Probability distribution functions of $\mathcal{M} \in \mathbb{C}$ obtained from 10^6 sweeps of SW on a lattice 8×8.

At low values of β (high temperature T) the system is found most probably in the disordered state $\mathcal{M} \approx 0$ and every spin state has equal probability. As the temperature lowers and approaches the critical point T_c, the probability distribution widens and takes the shape of a triangle oriented

as the magnetization domain. Finally, as we cross the critical point, the distribution becomes peaked around three different points situated along the directions of the cubic roots of the unity and representing high probabilities for configurations where a large number of spins are aligned. In the limit $\beta \to \infty$ ($T \to 0$) these points tend to the vertices of the triangle and the peaks of the probability distribution become very narrow.

1.6 Spatial Correlations

The two-point correlation function is defined as:

$$G(\vec{r}_i - \vec{r}_j) = \langle \mathrm{Re}(\sigma_i \sigma_j^*) \rangle \quad \sim \quad \exp(-|\vec{r}_i - \vec{r}_j| / \xi) \quad \text{for large} \quad |\vec{r}_i - \vec{r}_j| \tag{17}$$

where ξ is the correlation length of the system:

$$\xi = -\lim_{|\vec{r}| \to \infty} (|\vec{r}| / \ln G(\vec{r})) \tag{18}$$

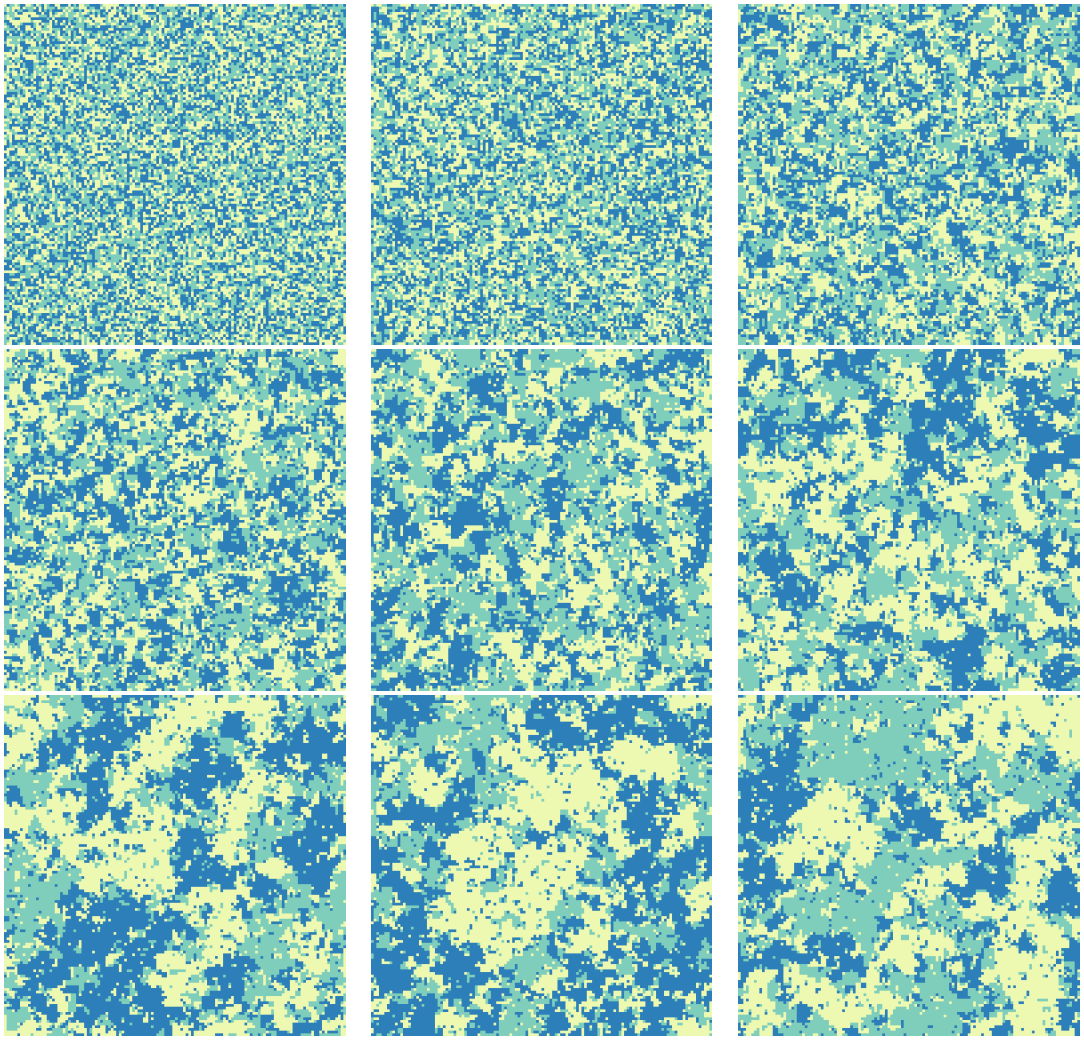

Figure 10. Ilustration of the growth of spatial correlations when criticality is approached on a lattice 128×128 : $\beta = 0.2, 0.5, 0.7, 0.8, 0.9, 0.95, 0.97, 0.98, 0.99$.

Analogously to the case of the Ising Model we define observables:

$$S_x \equiv \frac{1}{L}\sum_{y=1}^{L}\sigma(x,y) \tag{19}$$

$$S_y \equiv \frac{1}{L}\sum_{x=1}^{L}\sigma(x,y) \tag{20}$$

and we compute the correlation function as:

$$G(r) = \frac{1}{2}\left(\frac{1}{L}\sum_{x=1}^{L}\frac{S_x\,S^*_{x+r}}{S_x\,S^*_x} + \frac{1}{L}\sum_{y=1}^{L}\frac{S_y\,S^*_{y+r}}{S_y\,S^*_y}\right) \tag{21}$$

Again the fit is done via the hyperbolic cosine function:

$$G(r) \sim \frac{1}{2}\left(\mathrm{e}^{\frac{r}{\xi}} + \mathrm{e}^{\frac{L-r}{\xi}}\right) \sim \cosh\left(\frac{r-\frac{L}{2}}{\xi}\right) \tag{22}$$

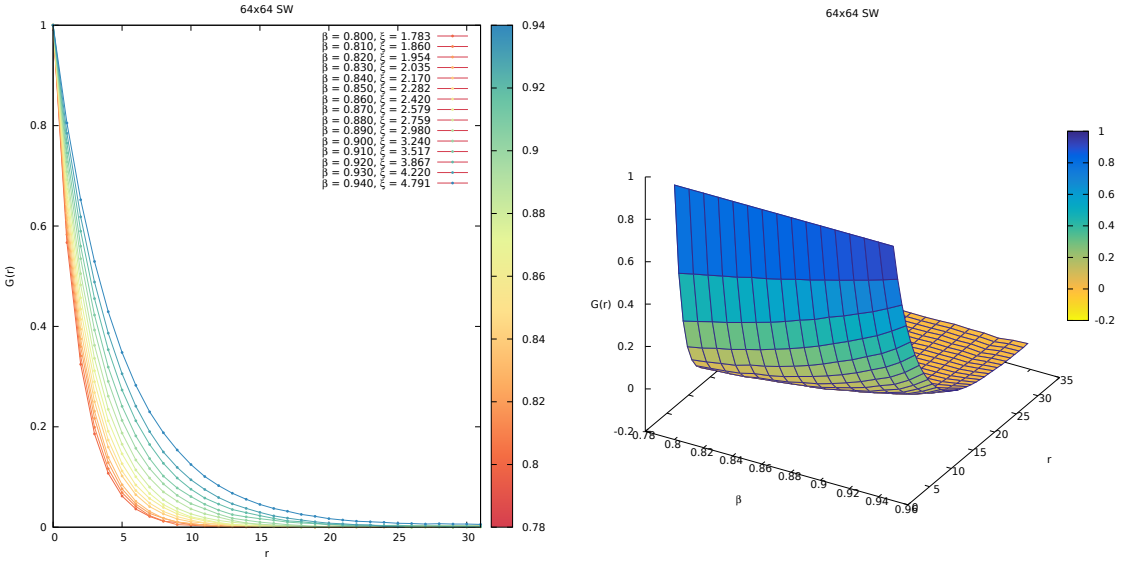

Figure 11. Correlation functions for various values of β. The lattice size used is 64×64. As a precaution, we considers an interval in β-space such that the correlation length is much smaller that the size of the lattice (approximately one order of magnitude smaller).

The correlation length diverges at the critical point as:

$$\xi \sim A\,|x|^{-\nu} \tag{23}$$

We plot the data obained from the previous fit using logarithmic scales on both axis and compute the critical exponent ν from the linear fit:

$$\log(\xi) = \log(A) - \nu\log(|x|) \tag{24}$$

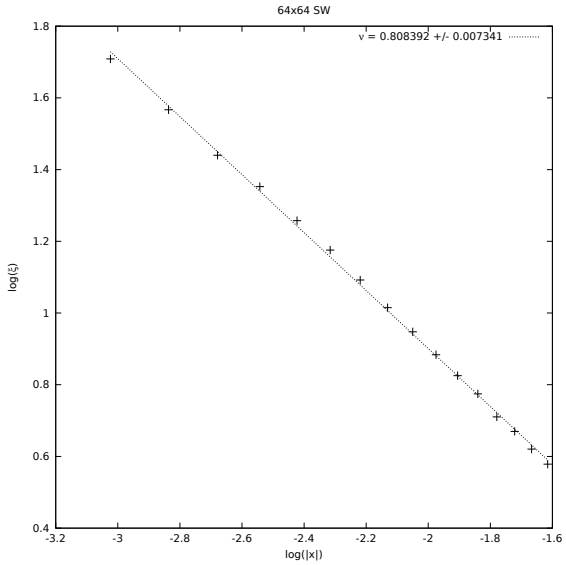

Figure 12. Plot of the correlation length dependence on the parameter $x = \frac{\beta - \beta_c}{\beta_c}$ for a lattice of size 64×64. The errors are computed by jackknife binning of the fit data from (Fig. 11).

The result of the fit is:

$$\nu_{\mathrm{SW}} = 0.80839 \pm 0.00734 \tag{25}$$

which is comparable with the exact value:

$$\nu = \frac{5}{6} \approx 0.83333...$$

1.7 Finite Size Scaling

The critical exponents of the model are:

ν	$5/6$
α	$1/3$
β	$1/9$
γ	$13/9$

Table 2. Exact critical exponents for the Potts model in $2d$.

We therefore rescale the observables as:

$$m \to m\, L^{\beta/\nu} \tag{26}$$

$$\chi \to \chi / L^{\gamma/\nu} \tag{27}$$

$$C \to C / L^{\alpha/\nu} \tag{28}$$

and plot the data expressed as function of the scaling variable $x\, L^{1/\nu}$:

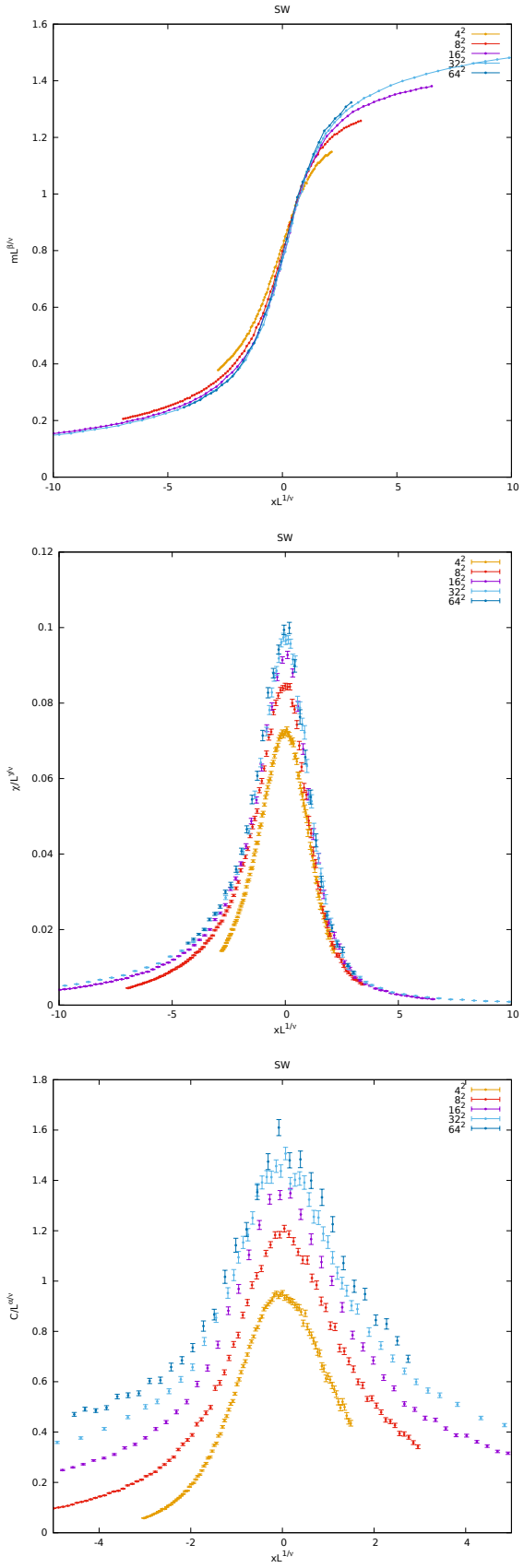

Figure 13. Finite Size Scaling study for the lattice sizes $4^2, 8^2, 16^2, 32^2$. The top plot represents the scaling of the magnetization, the center one the magnetic susceptibility and the bottom one the heat capacity.

Remark: the curves obtained by rescaling of the magnetization, susceptibility and heat capacity, fit well to the FSS functions $f_i\big(x\ L^{1/\nu}\big)$ when the system has a large enough volume that the boundary effects are nigligible. However, for smaller volumes ($L = 4, 8$) those effects are more important and, as we can se from (Fig.13), the fit becomes worse. In particular we see that the value $L = 4$ is too small for the scaling hypothesis to apply.